SCOPE | SAUDI INTERNATIONAL CONFERENCE ON NUCLEAR POWER ENGINEERING

Proceedings of SCOPE
13-15 Nov. 2023 – KFUPM
Paper 23131

# Towards the Development of a Comprehensive Nuclear System Analysis Code Based on Two-Fluid Model: Starting with an Isentropic Approach

Sultan Al-Faifi [a*]

[a]*King Abdullah City for Atomic and Renewable Energy, Riyadh 12244, Saudi Arabia*

**Corresponding author: s.faifi@energy.gov.sa*

**Abstract** - *In the complex field of nuclear reactor design and analysis, there is a continuous need for sophisticated computational models that can accurately capture the diverse and challenging thermal hydraulic phenomena during steady state and transient conditions. This research sets the stage for the development of a comprehensive system analysis code for nuclear reactor thermal hydraulic design, starting with a fully implicit isentropic two-fluid model with four governing equations. The computational methodology for this model incorporated the Advection Upstream Splitting Method (AUSM) scheme with a staggered grid arrangement. The nonlinear system of governing equations was solved implicitly by employing Newton's method while a numerical Jacobian matrix was calculated for the derivative terms, enhancing the stability and efficiency of the solution process. The performance of the model was assessed using three classical two-phase benchmark problems: water faucet problem, oscillating manometer problem, and air-water phase separation problem. The validation results indicate a reliable and accurate prediction of the model. Consequently, the successful development and validation of current two-fluid isentropic model provides a solid foundation for the future development of a comprehensive nuclear system analysis code based on the two-fluid model.*

**Keywords:** System Analysis Codes, Nuclear Thermal-Hydraulics, Two-Fluid Model, Fully Implicit Scheme

## I. Introduction

Nuclear reactors are complex engineering systems that require accurate understanding and prediction of neutronics and thermal hydraulics phenomena, which has a wide spectrum of interacting scales from microscopic to macroscopic. One of the crucial phenomena that occurs within these systems is two-phase flow, where two distinct phases, typically water and steam, coexist and interact dynamically. The accurate representation and prediction of such interactions is critical to the safety analyses of nuclear reactors.

Nuclear reactor system analysis codes such as RELAP5[1], TRAC [2], MARS[3], and SPACE[4], have been developed to capture the essential dynamics of two-phase flow in nuclear reactors. By using a one-dimensional two-phase two-fluid approach, they have achieved great success in supporting various nuclear applications, from safety evaluations of existing reactors to the design and licensing processes of new reactors. Their historical success illustrates the need and significance of comprehensive nuclear system analysis tools.

As the nuclear industry advances, there is a growing demand for more sophisticated numerical tools and methods to improve accuracy and computational efficiency. Furthermore, unavailability of source codes of all system analysis tools that are based on two-fluid approach adds significant limitations to users. This not only prevents the users from knowing the exact mechanism of the program but also reduces its flexibility, preventing the user from creating more customized models. As a result, the main objective of this paper is to set the stage for the development of a comprehensive nuclear system analysis tool, starting with a fully implicit isentropic two-fluid model with four governing equations.

## II. One-Dimentional Two-Phase Two-Fluid Model

The two-fluid, single-pressure, two-phase flow equations used in this study are similar to those found in the existing nuclear system analysis codes such as RELAP5, TRAC, TRACE, MARS, and SPACE. As an initial approach, the attention is focused on the isentropic two-phase two-fluid model, where the system of six equations is condensed to a set of four equations, as presented below:

$$\frac{\partial(\alpha_g \rho_g)}{\partial t} + \frac{\partial(\alpha_g \rho_g u_g)}{\partial x} = 0 \quad (1)$$

$$\frac{\partial(\alpha_l \rho_l)}{\partial t} + \frac{\partial(\alpha_l \rho_l u_l)}{\partial x} = 0 \quad (2)$$

$$\frac{\partial(\alpha_g \rho_g u_g)}{\partial t} + \frac{\partial(\alpha_g \rho_g u_g^2 + \alpha_g p)}{\partial x} = p\frac{\partial \alpha_g}{\partial x} \sigma \frac{\alpha_g \rho_g \alpha_l \rho_l}{\alpha_g \rho_l + \alpha_l \rho_g}(u_g - u_l)^2 \frac{\partial \alpha_g}{\partial x} + \alpha_g \rho_g g \sin(\theta) - C_f \alpha_g (1 - \alpha_g)\rho_g (u_g - u_l) \quad (3)$$

$$\frac{\partial(\alpha_l \rho_l u_l)}{\partial t} + \frac{\partial(\alpha_l \rho_l u_l^2 + \alpha_l p)}{\partial x} = p\frac{\partial \alpha_l}{\partial x} - \sigma \frac{\alpha_g \rho_g \alpha_l \rho_l}{\alpha_g \rho_l + \alpha_l \rho_g}(u_g - u_l)^2 \frac{\partial \alpha_l}{\partial x} + \alpha_l \rho_l g \sin(\theta) + C_f \alpha_g (1 - \alpha_g)\rho_g (u_g - u_l) \quad (4)$$

where the subscripts "l" and "g" correspond to the liquid and gas phases, respectively. For phase k, the terms in the equations above are defined as:

$\rho_k$ - density of phase k,

p - pressure,

$u_k$ - velocity of phase k,

$\alpha_k$ - volume fraction of phase k,

$C_f$ - interfacial drag coefficient,

g - gravitational constant

The first term in the mass conservation equations (1&2) refers to the mass rate of change of the control volume, while the second term refers to the flow of mass across the boundary of the control volume. For the momentum equations (3&4), the terms in the left-hand side represents the rate of change of the momentum of each phase and the change of the momentum and pressure across the boundaries of the control volume. In the right-hand side of Eq. (3) and (4), the first term represents momentum transfer due to the difference between average and interfacial pressure, the second term represents gravitational force and the third term represents the drag force per unit volume on the interfaces separating the two phases [5].

The variables derived from this set of equations include p, α, $u_l$, and $u_g$. These represent the pressure, void fraction (or the volume fraction of the gas phase), velocity of the liquid phase, and velocity of the gas phase, respectively. In order to obtain a closed system of governing equations, fluid properties are needed.

- Closure Equations:

The isentropic perfect gas and Tait's equations of state (EOS) serve as closure equations for the gas and liquid phases respectively [6]. Tait's EOS characterizes a liquid as compressible and barotropic, incorporating only pressure and density variables. Thus, when a liquid is modeled by this EOS, the energy equation is decoupled from the mass and momentum equations [7].

- Isentropic perfect gas EOS for the gas phase is expressed as:

$$p = p(\rho_g) = p_{g,0}\left(\frac{\rho_g}{\rho_{g,0}}\right)^{\gamma} \quad (5)$$

where $p^0_g = 10^5$ Pa, $\gamma = 1.4$ and $\rho^0_g = 1$ kg/m$^3$ .

Tait's EOS for the liquid phase, which is equivalent to linear secant-modulus equation [8], is given as:

$$p = p(\rho_l) = p_{l,0}\left[\left(\frac{\rho_l}{\rho_{l,0}}\right)^{n} - 1\right] \quad (6)$$

where

$p^0_l = 3.3 \times 10^8$ Pa, $n = 7.15$, $\rho^0_l = 1000$ kg/m$^3$ .

- The void fraction satisfies the following equation:

$$\alpha_g + \alpha_l = 1 \quad (7)$$

## III. Numerical and Solution Method

In this section, numerical method applied to the two-fluid model, as introduced in the first part of the paper, is discussed. The code was developed from scratch by the author, and a flowchart of the code is provided in Fig. 2.

The discretized equations were derived using a finite volume method on a staggered grid approach in order to avoid the commonly observed oscillations on pressure when collocated grids are used [9]. In this configuration, scalar quantities such as pressure, densities, and void fraction were assigned to cell centers, while velocities, as vector quantities, are defined at the cell boundaries. The spatial configuration is clearly shown in Fig. 1. The code is developed using a fully implicit scheme, ensuring unconditional stability in the numerical solution. This allows for stable numerical solution even with large time-steps, meaning the time-step is not constrained by the Courant limit (CFL).

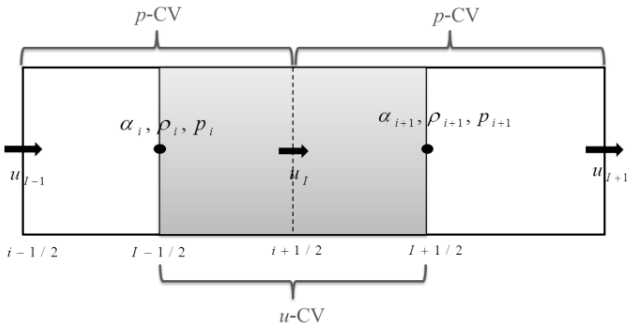


*Fig. 1. Staggered grids*

Using this as a foundation, the discretized equations were formulated in residual form. It should be noted that in the following equations, the superscripts "n" and "n + 1" differentiate between time steps, while subscripts marked with "i" and "I" indicate spatial positioning of scalar and vector control volumes, respectively.

The discretized governing equations can be expressed in the following vector form:

$$\boldsymbol{R}(\boldsymbol{w}) = 0 \qquad (8)$$

where **R** is the residual vector of the system.

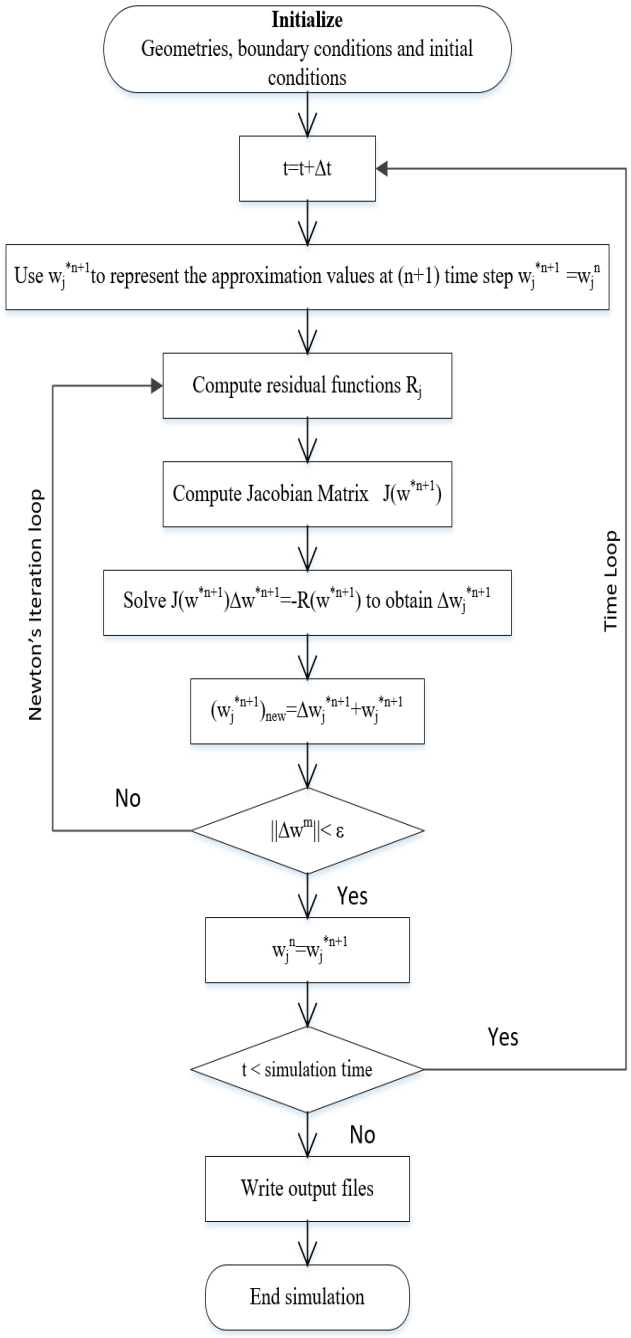


*Fig. 2. Flow chart of the two fluid code with an implicit time integration method.*

The residuals of the fully implicit discretized mass conservation equations for the two phases are as follows.

$$R_{1,i} = (\alpha_g \rho_g)_i^{n+1} - (\alpha_g \rho_g)_i^{n} + \frac{\Delta t}{\Delta x}\left[(f_g)_{i+\frac{1}{2}}^{n+1} - (f_g)_{i-\frac{1}{2}}^{n+1}\right] \quad (9)$$

$$R_{2,i} = (\alpha_l \rho_l)_i^{n+1} - (\alpha_l \rho_l)_i^{n} + \frac{\Delta t}{\Delta x}\left[(f_l)_{i+\frac{1}{2}}^{n+1} - (f_l)_{i-\frac{1}{2}}^{n+1}\right] \quad (10)$$

where $(f_k)_{i+1/2} = \left((\alpha_k \dot{\rho}_k)\, u_k\right)_{i+1/2}$ is the mass flux of the k[th] phase at i + 1/2 location.

The residuals of the fully implicit discretized momentum equations are as follows.

$$R_{3,I} = \left(\widetilde{\alpha_g}\widetilde{\rho_g} u_g\right)_I^{n+1} - \left(\widetilde{\alpha_g}\widetilde{\rho_g} u_g\right)_I^{n} + \frac{\Delta t}{\Delta x}\left[(f_g)_{I+\frac{1}{2}}^{n+1} - (f_g)_{I-\frac{1}{2}}^{n+1}\right] - (\tilde{p}_{int})_I^{n+1}\frac{\left[(\alpha_g)_{i+1}^{n+1} - (\alpha_g)_i^{n+1}\right]}{\Delta x} - \left(\widetilde{\alpha_g}\widetilde{\rho_g} g\right)_I^{n+1} \quad (11)$$

$$R_{4,I} = (\widetilde{\alpha_l}\widetilde{\rho_l} u_l)_I^{n+1} - (\widetilde{\alpha_l}\widetilde{\rho_l} u_l)_I^{n} + \frac{\Delta t}{\Delta x}\left[(f_l)_{I+\frac{1}{2}}^{n+1} - (f_l)_{I-\frac{1}{2}}^{n+1}\right] - (\tilde{p}_{int})_I^{n+1}\frac{\left[(\alpha_l)_{i+1}^{n+1} - (\alpha_l)_i^{n+1}\right]}{\Delta x} - (\widetilde{\alpha_l}\widetilde{\rho_l} g)_I^{n+1} \quad (12)$$

Where $(f_k)_{I+1/2} = \left(\alpha_k \rho_k \dot{u_k}^2 + \alpha_k p\right)_{I+1/2}$ is the momentum flux of the k[th] phase at I+1/2 location.

Scalar properties such as pressure, density, and void fraction are defined at cell centers. To calculate numerical fluxes, values for these properties are required at cell interfaces. These are represented as variables with a "dot" in fluxes of equations (9) & (10). In RELAP5 nomenclature, these quantities are referred to as 'donored' quantities. The same principle applies to momentum numerical fluxes in equations (11) and (12), where velocities need to be available at cell centers. The order of accuracy for our discretization depends on the method used to calculate these donored quantities in numerical fluxes.

The system of equations (9)-(12) contains four primitive variables: P, $u_l$, $u_g$, $\alpha_g$; which are solved by applying the Newton-Raphson method, as follows.

$$\left(\frac{\partial \boldsymbol{R}}{\partial \mathbf{w}}\right)^m \Delta \boldsymbol{w}^m = \boldsymbol{R}(\boldsymbol{w}^m) \quad (13)$$

By solving Eq. (13), one can obtain the increment Δw at the m[th] iteration. In turn, the variable vector **w** at the (m + 1)[th] iteration is given by Eq. (14).

$$\boldsymbol{w}^{m+1} = \boldsymbol{w}^m + \Delta \boldsymbol{w}^m \quad (14)$$

where $\mathbf{w}^{m+1}$ is the solution of Eq. (8) when the $l_2$-norm of $\Delta\mathbf{w}^m$ satisfies the following criteria:

$$\|\boldsymbol{w}^m\| < \boldsymbol{\varepsilon} \quad (15)$$

where ε is the tolerance, $\varepsilon = 10^{-4}$.

The numerical Jacobian calculation, which will be used for the derivative term in Eq. (13), can be calculated as follows [10].

$$\left(\frac{\partial \boldsymbol{R}}{\partial \mathbf{w}}\right)^m = \frac{\boldsymbol{R}(\boldsymbol{w}^m + \boldsymbol{\varepsilon e}) - \boldsymbol{R}(\boldsymbol{w}^m)}{\boldsymbol{\varepsilon}} \quad (16)$$

## IV. Test Results

### *IV. A. Ransom's water faucet problem*

The two-phase water faucet problem, initially proposed by Ransom [11], stands as an excellent benchmark problem for two-phase flow dynamics. This problem, along with its analytical solution, has been extensively employed in the nuclear scientific community for code validation, benchmarking, and numerical accuracy assessments. It provides an analytical representation of the gravitationally-induced acceleration of a liquid column. As illustrated in Fig. 3, a vertical pipe of 12 meters in length is initially filled with a uniform column of water surrounded by annulus of air moving in downward direction at a constant speed of 10 m/s. Under the influence of gravitational forces, the liquid phase undergoes acceleration, consequently resulting in a contraction of the water jet over time in order to satisfy

the mass conservation equation. This transient state continues until the contact discontinuity (i.e. void wave) leaves the system, resulting in a steady-state condition. The initial states are given by

$$(\alpha_g, u_g, u_l, p) = (0.2, 0\ \text{m/s}, 10\ \text{m/s}, 10^5\ \text{P a}) \quad (17)$$

The inlet boundary condition is set to be the same as Eq. (17), except for the pressure, which is extrapolated from the interior node. On the contrary, for the outlet boundary condition, the pressure is imposed to be $10^5$ Pa and the other variables are extrapolated from within the computational domain. When solving the problem implicitly, the tolerance ε in the Newton's loop is set to be $10^{-4}$. Perturbation value $\varepsilon_i = 10^{-6}$ for all primitive variables.

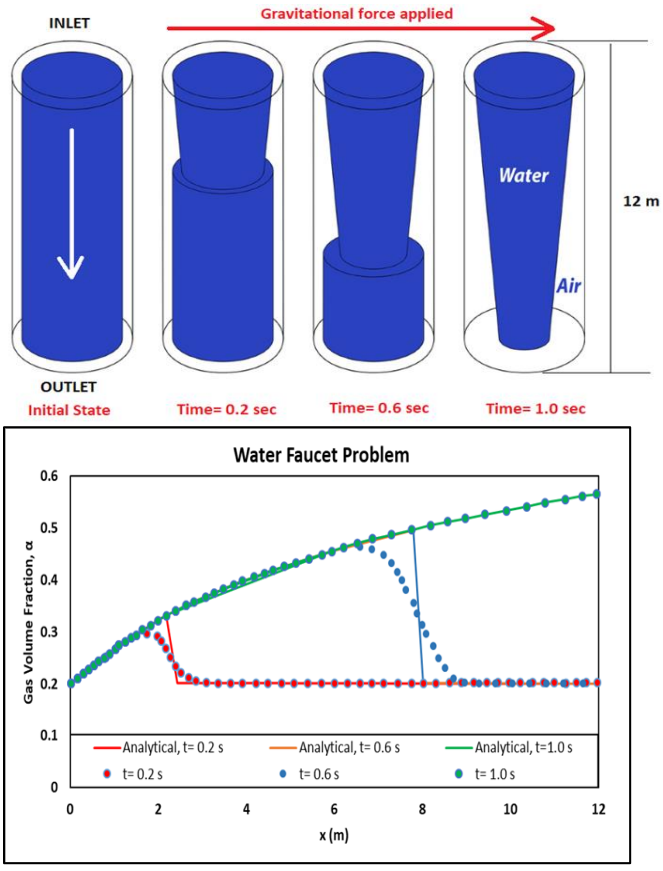


*Fig. 3. Water Faucet Problem*

Fig. 3 shows the numerical results of the void fraction distribution compared to analytical results at 0.2 s, 0.6 s, and 1.0s. The numerical results align closely with the analytical solution with a stable calculation.

### IV. B. Manometer Oscillation Problem

The oscillatory manometer problem was initially introduced as a benchmark problem for two-phase flow analyses [12]. In this scenario, a U-shaped tube with a total length of 20 m is examined. Initially, the U-tube manometer contains both gas and water, with the water moving at a uniform velocity of 2.1 m/s. The U-shaped manometer is half-filled with water, as illustrated in Fig. 4.

This test serves as a benchmark for the computational modeling of inertial and body force effects. It also serves to test the ability of numerical schemes to simulate the oscillations of the liquid-gas interface.

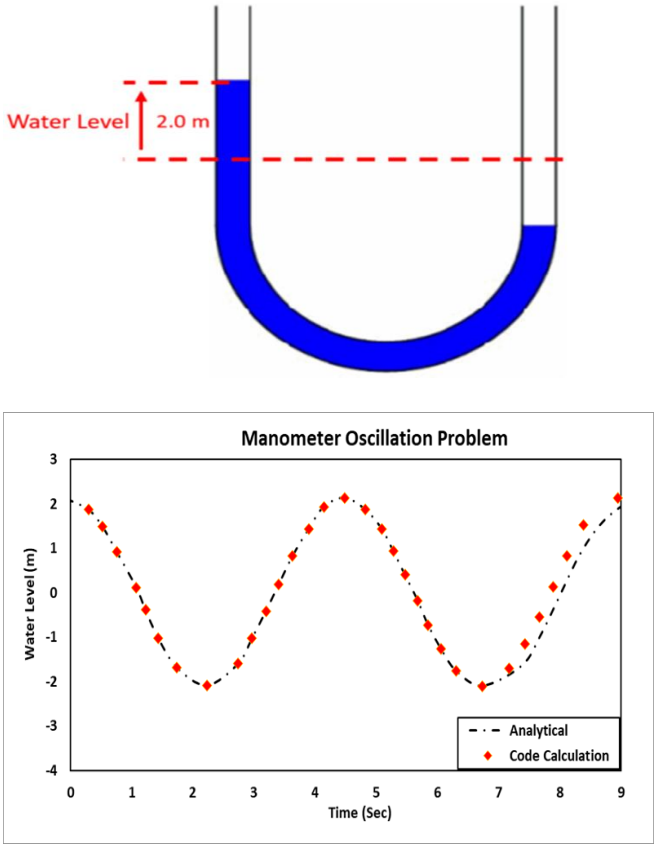


*Fig. 4. Manometer oscillation problem*

Fig. 4 shows numerical results of the liquid levels in the left leg of the U-shaped manometer. The liquid level was determined by calculating the total liquid volume in the left part of the tube. The results shown in the figure closely match the analytical solution, with excellent agreement in tracking the oscillation magnitudes of the water level.

### *IV. C. Phase separation problem*

The sedimentation problem proposed by Coquel [13], serves as a test to examine phase separation influenced by gravitational forces. This test involves a vertical pipe initially filled with a two-phase mixture with a uniform void fraction of $\alpha_g$= 0.5. Under gravitational influence, the two phases separate, resulting in the denser liquid phase settling at the pipe's base and the lighter phase rising to its top. This test assumes no mass transfer. Fig. 5 provides a schematic representation of the sedimentation problem. There are two numerical challenges in the simulation of the sedimentation test, 1) a dynamically developed phase disappearance phenomenon due to phase separation; and 2) a sharp interface existing between the separated two phases.

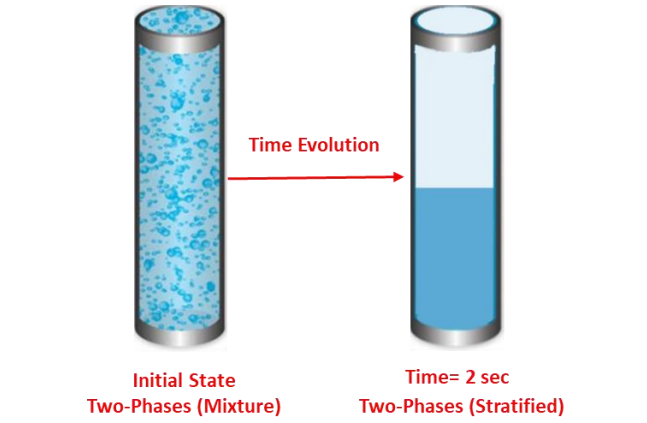


*Fig. 5. Phase separation problem*

Fig. 5 shows the transient distribution of void fraction throughout the pipe. Two distinct void fronts are observed, moving in opposite directions - one upward and one downward eventually converging near the pipe's center after 2 sec. The numerical results align closely with the analytical solution.

## VII. Conclusion

In conclusion, the complex field of nuclear reactor design and analysis presents many challenges that require advanced numerical tools to accurately capture thermal hydraulic phenomena during both steady state and transient phases. The foundation has been laid in this research for a thorough system analysis code essential for nuclear reactor thermal hydraulic design, with the primary focus on an implicitly solved isentropic two-fluid model. The computational approach adopted, integrating the Advection Upstream Splitting Method (AUSM) with a staggered grid, demonstrated significant promise. By using Newton's method for the implicit solution of the governing equations and computing a numerical Jacobian matrix for the derivatives, both of solution stability and efficiency were achieved. This study introduced three test problems to validate the proposed numerical tool: the water faucet problem, the oscillating manometer problem, and the phase separation problem. The benchmark validation results highlight the code's stability and precision in its predictions. Therefore, the successful implementation of the two-fluid isentropic model establishes a solid foundation for the future development of a comprehensive nuclear system analysis code based on the fully implicit two-fluid model.

## References

1) RELAP5/MOD3.3 Code Manual Volume I, December 2001. NUREG/CR-5535 ed., U.S.Nuclear Regulatory Commission.
2) TRAC-M/FORTRAN 90 (Version 3.0) Theory Manual, April 2001. NUREG/CR-6724 ed., U.S. Nuclear Regulatory Commission.
3) Chung, B. D., Kim, K. D., Bae, S. W., Jeong, J. J., Lee, S. W., Hwang, M. K., & Yoon, C. (2010). MARS code manual volume I: code structure, system models, and solution methods (No. KAERI/TR--2812/2004). Korea Atomic Energy Research Institute.
4) Ha, S. J., Park, C. E., Kim, K. D., & Ban, C. H. (2011). Development of the SPACE code for nuclear power plants. Nuclear Engineering and Technology, 43(1), 45-62.

5) Hibiki, T., Ishii, M., 2006. Thermo-fluid dynamics of two-phase flow. Springer.
6) H. Paill`ere, C. Corre, and J. Garcıa Cascales, "On the extension of the AUSM+ schemeto compressible two-fluid models," Computers & Fluids, vol. 32, no. 6, pp. 891–916, 2003.
7) Qiulan Zeng (2017). Numerical Schemes for 1-D Two-Phase Flows. UWSpace.
8) Hayward, A. (2002). Compressibility equations for liquids: A comparative study. British Journal of Applied Physics. 18. 965. 10.1088/0508-3443/18/7/312.
9) Prosperetti, A., Tryggvason, G., 2009. Computational methods for multiphase flow. Cambridge university press.
10) Onur O, Eyi S. Effects of the Jacobian evaluation on Newton's solution of the Euler equations. International Journal for Numerical Methods in Fluids 2005; 49(2):211–231.
11) Ransom, V.H., 1987. Numerical benchmarck test no 2.1: Faucet flow. Multiphase Science and Technology3, 465–467.
12) Hewitt, G. F., Delhaye, J. M., Zuber, N. 1987. Multiphase Science and Technology
13) Coquel F, El Amine K, Godlewski E, Perthame B, Rascle P. A numerical method using upwind schemes for the resolution of two-phase flows. Journal of Computational Physics 1997; 136(2):272–288.